Relaxation modelling of surfactants in aqueous solutions

Pau Mayorga Delgado
2548586
University of Oulu
Faculty of science
08/2020

Contents

1 Introduction

Nuclear Magnetic Resonance (NMR) is a field of science that studies the properties of matter in both microscopic and macroscopic level through magnetic interactions with the atomic nuclei's magnetic moment.[Keeler, 2011][Jozef Kowalewski, 2006]

The main goal of this thesis is to theoretically develop and examine the determination of the diffusion coefficient, to gain an understanding at a molecular level via computational simulations. The system considered is the surfactant Sodium Dodecyl Sulfate (SDS) in water, which is the active ingredient of soap. The experimental observables are from NMR diffusion and relaxation measurements.

There are already many successful studies concerning the study of SDS, such as [Yuan et al., 2001]. In there, it is determined the SDS experimental diffusion coefficient in water and the transversal relaxation time within a certain SDS concentration range. The former describes the movement of molecules or particles in the media, while the latter characterizes the rate at which the magnetizations returns to its equilibrium.

In [Yuan et al., 2001] the experimental diffusion and the transversal relaxation rates at low concentrations are constant. These rates are explained by a monomer state at concentrations below the critical micelle concentration (CMC), where larger aggregates are formed. A conformation and motivation of this monomer hypothesis is needed with a description at microscopical level. The reason for this is that these two observables (diffusion and relaxation) are highly related to the interaction of the molecules between themselves and with the medium. Also the geometry of the molecule has a strong effect in those parameters. These are reasons which makes it natural to use computer simulations to get the theoretical parameters. With the simulation methodology of this work we are able to quantitatively discuss the experimental results of [Yuan et al., 2001].

A way of determining the theoretical SDS diffusion coefficient and the relaxation times are through molecular dynamic simulations [Case et al., 2016], which allows us to take into consideration every single atom interaction with the neighbouring atoms within a time scale suitable for even the fastest motions, such as the H-O vibration (time scale of a few femtoseconds). On the other hand, those simulations can take a couple of days with 24 processors, which means that this process is really time consuming and require simulation resources, specially if it is intended to simulate bigger aggregates.

An alternative to that would be, to determine the observables by using the molecule hydrodynamic radius in the Stokes-Einstein equation (SE) [Edward, 1970, p.261]. That way it would be possible to obtain the theoretical values of the SDS diffusion and relaxation times straight by substitution in the SE equation instead of by spending a considerable amount of hours of simulation to obtain the molecule's Mean Square Displacement through which the theoretical diffusion can be obtained as well. The problem with that hydrodynamic radius is that it has several limitations, like considering the

molecules as a perfect and rigid spheres, when it is not the case.

In this work it is studied the possibility of using the hydrodynamic radius of the SDS molecule, by comparing the theoretical results obtained with the Stokes-Einstein equation, and the results obtained by using a molecular dynamic simulation. The intention is to extend this work to the study of SDS aggregate (micelles) formation in water, because this would help to get a better understanding of the aerosol impact in the climate. [NASA earth observatory, 2010]

This thesis starts by an introduction of surfactants (Section 2), such as the SDS, and its possible aggregates with their properties, since it is important to have a general idea of the macroscopic behaviour in water of these compounds. After that there is an introduction of NMR and relaxation theory (Section 3), aiming to explain important concepts like *correlation function* and *spectral density function* and how they come about [Keeler, 2011, p.253 and p.256-258], in order to use them later on to explain the SDS diffusion and justify the use of the hydrodynamic radius. Next, it is discussed where the diffusion coefficient comes from and the dispute with the Stokes-Einstein's equation as well as the types of hydrodynamic radii (Section 4). To finish this thesis's theoretical section, it is introduced some molecular dynamic simulation techniques and considerations (Section 5), to get the MSD from the studied molecule and study its behaviour by using the theory. Finally the results obtained from the simulations are presented as examples (Section 6) and conclusions are drawn (Section 7), with the possibility of extending this work in the future.

2 Surfactants

A surfactant has a head group that attracts water molecules (hydrophilic) and a carbon chain that repels them (hydrophobic). This types of molecules with the two groups are called amphiphilic. In an aqueous solution these amphiphilic molecules reorganize themselves forming a sphere shaped aggregate known as micelles, with the hydrophobic group inwards. They can also form other structures such as cylinders or bilayers.[Wennerström, 1999, p.5]

Even though this thesis focuses in the study of a low concentration of SDS molecule in water, it is also important to have a more general picture of what direction this work might take in the future. Thus, it is essential to describe what kind of structures this lipid can form at higher concentrations and its basic properties.

The word surfactant comes from *surface active agent* because they lower the surface tension between two phases, and in the case of SDS solution in water, between water and air. The reason behind this is that the insolubility of the hydrophobic tail in water causes the molecule to concentrate in the interface with the tail oriented towards the vapour phase. Because the water surface tension is higher than the surfactant's, by adding the amphiphilic molecule the surface tension of the solution decreases.[Wennerström, 1999, p.8]

When a certain surfactant is added into water, the solution's surface tension decreases until the surfactant starts forming micelles. After this point the surface tension remains almost constant and the surfactant it is said to have reached the *critical micelle concentration* (CMC). This is an informative parameter to follow in the study of micelle formation. In this thesis we have really low surfactant concentration and thus, it is considered that the system is all the time below the CMC. In [Wennerström, 1999, pp.8-9] it is stated that as more surfactant is added into water after the CMC has been reached, it will just form more micelles instead growing in size the existing ones. As an example is given the case of the SDS molecule, which CMC in water at 20 °C is $8.1 \cdot 10^{-3}$M and the SDS micelles contain approximately 60 SDS molecules.

Another factor that affects to the micelle formation is the temperature. At low temperature, the surfactant precipitates in form of crystals instead of forming micelles. The temperature from which the surfactant is able to form micelles and therefore the CMC is equal to the surfactant's solubility is known as *Krafft temperature* (T_{Kr}). The Krafft temperature for the SDS is about 22 °C.[Wennerström, 1999, pp.10-11]

The *surfactant packing parameter*,

$$N_{\mathrm{s}} = \frac{v}{la_0}, \tag{1}$$

provides a guide for the preferred curvature properties that the aggregates will have. In Eq. (1), v is the volume of the hydrophobic chain of the surfactant molecule, l is

the maximum length in nanometres of a fully extended hydrocarbon chain and a_0 is the effective area per head group. For small N_s the surfactant form aggregates with really curved surfaces. For example, when $N_s = 0.33$, the surfactants form spherical micelles, such as for the SDS molecules, and, for $N_s = 0.5$, there is a preference for infinite cylinders. For bigger N_s, the aggregates tend to flatten out until $N_s = 1$, which would form planar bilayers. For $N_s > 1$, the surfactant forms inverted cylinders and micelles and in that case the solvent would be organic.[Wennerström, 1999, pp.14-18]

3 Basics of NMR spectroscopy and relaxation

This chapter is focused mainly on describing the relaxation phenomena and its mechanisms, and it ends with a description and derivation of the main relaxation parameters, T_1 and T_2.

NMR is a phenomenon that occurs when atomic nuclei are within a certain applied magnetic field, and a radio frequency beam is used to disrupt the alignment of nuclei from the applied field direction. The detection of the nuclei's signal takes place through a coil surrounding the sample, which detects the nuclei's magnetic momentum precessing the applied field after the RF beam.

The nuclei interact with the static magnetic field, because they have a spin angular momentum, which is associated with the nuclear spin magnetic moment. Once an external magnetic field is placed, the generated magnetic field from the nucleus interacts with it. [Joseph P. Hornak, 1997]

3.1 Basics on relaxation

It is important to stress the connection between MD simulations and relaxation. In the former, all the distances and interactions between all the atoms are taken into account for every time step. The latter has certain mechanisms, such as the dipolar interaction explained in the Section 3.6, which can make use of those distances obtained from the MD simulations and extract the system's dimension and geometry. Therefore it's really important to have some notions of this relaxation phenomena, which is the goal of this section.

Relaxation is a mechanism by which the bulk magnetization, which is the net sum of all the nuclei's magnetic moments, goes back to its equilibrium position after having been disrupted from its equilibrium state. Thus, the bulk magnetization returns to its minimum energy state, aligned with the magnetic field. This means that if the static magnetic field is pointing along certain axis, say z, the bulk magnetization will reach a steady value along z over time, and at the same time, the transverse magnetization, along the xy axis, goes to zero as it is visualized in Figure 1, in which the z-magnetization equilibrium is represented by a dashed line. This can be a relatively slow process which can take even minutes in extreme cases. [Keeler, 2011, pp.241-242]

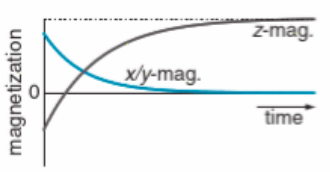

Figure 1: z- and x/y-magnetization. [Keeler, 2011, p.242]

The interaction energy between the spin and the static magnetic field becomes smaller as the angle between them decreases. On the other hand, these interactions are quite feeble compared to the thermal energy of the molecules, and therefore this last

one disturbs the alignments between the spins and the static magnetic fields. Regardless of the thermal motion, there is a favourable minimum energy state which makes that spins tend to align within static magnetic field. Because of that, the average magnetic moment over the sample is somewhat aligned with the external magnetic field and then it is said that the sample is magnetized, which is represented by a bulk magnetization vector. The word bulk makes reference to the whole sample. [Keeler, 2011, pp.47-48]

As previously stated, in order to observe the relaxation phenomena, it is needed first that the z-magnetization is disrupted from its equilibrium state. This can happen by applying a radio-frequency (RF) pulse. When a RF pulse is applied to the sample in its equilibrium state, the magnetization vector is spun towards the xy-plane and, as a consequence, it decreases in size in the z-direction and the produced transverse magnetization precesses at the Larmor frequency about the external magnetic field. This precession is what is detected as a free induction decay (FID). [Keeler, 2011, p.243]

The bulk magnetization can be rotated from the z-axis direction at the Larmor frequency just with a RF-pulse. On the other hand, the bulk magnetization vector length along the z-axis can decrease naturally as a consequence of the interaction between each of the individual spin magnetic moments. Because each spin has its own magnetic field, spins experience not only the applied external field but also the field from other neighbour spins. This field is called *local field* and is much weaker than the external field. The effect of the local field within the sample is greatly localized and these are the cause of the bulk magnetization to go towards its equilibrium state. [Keeler, 2011, p.244]

As it can be observed in the picture (Figure 2), the spin energy increases when the bulk magnetization is moved from the z-axis, and, in order for spins to go back to equilibrium, they need to give up energy, although this amount of energy is really small compared with the energy from the thermal motion. The mechanism through which the z-magnetization is returned to the equilibrium is called *longitudinal relaxation* with characteristic time T_1 and the process by which the transverse or xy-magnetization decreases to zero is called *transverse relaxation* with characteristic time T_2. [Keeler, 2011, pp.246-247]

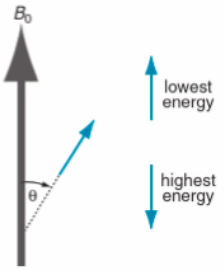

Figure 2: Angle dependency of the bulk magnetization vector to the applied field (B_0). [Keeler, 2011, p.47]

3.2 Longitudinal relaxation

Although the magnetic moment of a spin-half nucleus can point in any direction in space and its energy depends on the angle between its magnetic moment and the

applied magnetic field, when that energy is actually measured, just two possibilities arise, one for the energy level associated to the spin at the state α and another one for the state β. Therefore the probability of finding a spin in the α state is p_α and for the β state p_β. Hence the population of a certain state is defined as the sum of the probabilities of finding the spin at that state over the whole sample,

$$n_\alpha = \sum_{i=1}^{N} p_{\alpha,i}, \tag{2}$$

where N is the number of spins in the sample. [Keeler, 2011, pp.258-259]

In order to determinate the bulk z-magnetization of a sample, it is needed to take into account that a spin in the α state adds to the z-magnetization to a factor of $\frac{1}{2}\hbar\gamma$ and in the case of a spin in the β state its addition to the z-magnetization is of $-\frac{1}{2}\hbar\gamma$. Therefore the bulk magnetization expressed in spin populations can be described as

$$M_z = \frac{1}{2}\hbar\gamma(n_\alpha - n_\beta). \tag{3}$$

In other words, the bulk z-magnetization is proportional to the difference between the spin population states. [Keeler, 2011, p.259]

It is well known that at equilibrium the populations follow the Boltzmann distribution and therefore

$$\begin{cases} n_\alpha^0 = \frac{1}{q}N\exp(\frac{-E_\alpha}{k_BT}) = \frac{1}{2}N\exp(\frac{-E_\alpha}{k_BT}) \\ n_\beta^0 = \frac{1}{q}N\exp(\frac{-E_\beta}{k_BT}) = \frac{1}{2}N\exp(\frac{-E_\beta}{k_BT}), \end{cases} \tag{4}$$

where n_α^0 and n_β^0 are the populations at the state α and β respectively, q is the partition function but in this case $q = 2$ because there are just two possible states, $E_{\alpha/\beta}$ are the energies for each state and k_B is the Boltzmann's constant. As $E_{\alpha/\beta} << k_BT$, $\frac{E_{\alpha/\beta}}{K_BT} << 1$ and hence a Taylor expansion can be applied for the population as follows:

$$\begin{cases} n_\alpha^0 = \frac{1}{2}N\exp(\frac{-E_\alpha}{K_BT}) \approx \frac{1}{2}N(1 - \frac{E_\alpha}{K_BT}) \\ n_\beta^0 = \frac{1}{2}N\exp(\frac{-E_\beta}{K_BT}) \approx \frac{1}{2}N(1 - \frac{E_\beta}{K_BT}) \end{cases} \tag{5}$$

From here the bulk z-magnetization at the equilibrium can be easily obtained by pure substitution,

$$M_z^0 = \frac{1}{2}\hbar\gamma(n_\alpha^0 - n_\beta^0) = \frac{1}{4}\hbar\gamma N\frac{E_\beta - E_\alpha}{k_BT}. \tag{6}$$

These energies are proportional to the applied fields as follows: $E_\beta = \frac{1}{2}\hbar\gamma B_0$ and

$E_\alpha = -\frac{1}{2}\hbar\gamma B_0$ and by substitution again is obtained the following expression

$$M_z^0 = \frac{\gamma^2\hbar^2 N B_0}{4k_B T}. \tag{7}$$

[Keeler, 2011, pp.259-260]

Considering the proportionality $M_z \propto n_\alpha - n_\beta$, it can be seen that a spin transition from α to β decreases the population change and therefore M_z gets smaller. Analogously, a spin transition from β to α increases the population change and M_z increases. It can therefore be established that the rate of change of the spin from α to β is $W_{\alpha\to\beta}n_\alpha$, where $W_{\alpha\to\beta}$ is a rate constant, and analogously from β to α is $W_{\beta\to\alpha}n_\beta$.

The same expressions can be written using the deviation of the population with the equilibrium. With that, the new expression for the rate of change of a spin from α to β is $W_{\alpha\to\beta}(n_\alpha - n_\alpha^0)$ and from β to α is $W_{\beta\to\alpha}(n_\beta - n_\beta^0)$. The first expression is a rate of n_α decrease and the second expression by how much n_β decreases, or what is the same, by how much n_α increases. From here it can be written the rate of change on n_α and n_β as

$$\begin{cases} \frac{dn_\alpha}{dt} = W_{\alpha\beta}(n_\beta - n_\beta^0) - W_{\alpha\beta}(n_\alpha - n_\alpha^0) \\ \frac{dn_\beta}{dt} = W_{\alpha\beta}(n_\alpha - n_\alpha^0) - W_{\alpha\beta}(n_\beta - n_\beta^0), \end{cases} \tag{8}$$

where it has been assumed that $W_{\alpha\to\beta} = W_{\beta\to\alpha} = W_{\alpha\beta}$.[Keeler, 2011, pp.261-262]

Before it was stated that the bulk z-magnetization could be roughly written as $M_z = n_\alpha - n_\beta$ [Keeler, 2011, p.260]. Therefore the rate of change of M_z using derivatives can be written analogously as

$$\begin{aligned} &\frac{dM_z}{dt} = \frac{dn_\alpha}{dt} - \frac{dn_\beta}{dt} = (W_{\alpha\beta}(n_\beta - n_\beta^0) - W_{\alpha\beta}(n_\alpha - n_\alpha^0)) - \\ &(W_{\alpha\beta}(n_\alpha - n_\alpha^0) - W_{\alpha\beta}(n_\beta - n_\beta^0)) = 2W_{\alpha\beta}(n_\beta - n_\beta^0) - 2W_{\alpha\beta}(n_\alpha - n_\alpha^0) = \\ &- 2W_{\alpha\beta}[(n_\alpha - n_\beta) - (n_\alpha^0 - n_\beta^0)] = -2W_{\alpha\beta}(M_z - M_z^0). \end{aligned} \tag{9}$$

For longitudinal relaxation it is often written that $\frac{dM_z}{dt} = -\frac{1}{T_1}(M_z - M_z^0)$, where $T_1 = \frac{1}{2W_{\alpha\beta}} = \frac{1}{R_z}$ is the time constant called T_1 *relaxation time*. [Keeler, 2011, p.262]

3.3 Transverse relaxation

Supposing that the longitudinal relaxation is along the z-axis and as it has been described in a previous section, the transverse relaxation is the process or mechanism by which the xy-magnetization or transverse magnetization decreases to zero. The main idea is that each spin in the sample will interact up to a certain degree with each other and their precession along the applied field will be less coordinated, meaning that they will dephase. This lack of coordination causes that over time the average

xy-magnetization from the whole sample will tend to zero. [Keeler, 2011, p.248]

Analogously to the longitudinal relaxation, the transverse relaxation can be expressed by the following equation:

$$\frac{dM_{x/y}(t)}{dt} = -R_{xy}M_{x/y}(t), \tag{10}$$

where R_{xy} is the transverse constant rate, $M_{x/y}$ is the x or y magnetization and its value at the equilibrium is zero. For simplicity, from now on the x-magnetization (M_x) will be used but the same is applied for the M_y.[Keeler, 2011, p.293]

By solving this differential equation it is obtained that $\ln(M_x(t)) = -R_{xy}t + C$, where C can be found by setting $t = 0$ and therefore $C = \ln(M_x(0))$. By rearranging we get

$$M_x(t) = M_x(0)\exp(-R_{xy}t), \tag{11}$$

where it is quite clear that as time increases, the x-magnetization gets smaller towards zero from an initial $M_x(0)$. The constant R_{xy} is commonly known as $R_{xy} = \frac{1}{T_2}$, where T_2 is known as T_2 *relaxation time*. [Keeler, 2011, pp.293-294]

3.4 Relaxation times for the fast motion regime

Since the SDS molecule is in the fast motion regime as showed in Section 6.2 in the results chapter, it is valuable to introduce a way to calculate the relaxation times T_1 and T_2 from experimental or simulated data in a simplified form.

The general expressions for the proton T_1 and T_2 are:

$$T_1^{-1} = \frac{1}{5}I(I+1)\left(\frac{\mu_0^2\gamma^4\hbar^2}{16\pi^2 r_{\text{eff}}^6}\right)\Big[j(\omega_0) + 4j(2\omega_0)\Big] \tag{12}$$

and

$$T_2^{-1} = \frac{1}{5}I(I+1)\left(\frac{\mu_0^2\gamma^4\hbar^2}{16\pi^2 r_{\text{eff}}^6}\right)\Big[\frac{3}{2}j(0) + \frac{5}{2}j(\omega_0) + j(2\omega_0)\Big], \tag{13}$$

where $I = \frac{1}{2}$ is the proton's spin quantum number, j is the reduced spectral density at $\omega = 0$, at Larmor frequency and at two times the Larmor frequency, and r_{eff} is the effective distance between the reference protons and the rest of the protons in the molecule. It needs to be pointed out, that for the fast motion regime $j(0) = j(\omega_0) = j(2\omega_0) = 2\tau_c$ according to the Eq. 20 in the next section, and thus,

$$T_1^{-1} = T_2^{-1} = \frac{3}{4}\frac{\mu_0^2\gamma^4\hbar^2}{8\pi^2 r_{\text{eff}}^6}\tau_c \tag{14}$$

[Jozef Kowalewski, 2006, p.41,57] [Zhao and Fung, 1993].

3.5 Time correlation function

The time correlation function (TCF) is the average over the whole sample of the local fields at time t multiplied by the local field at time τ,

$$G(t,\tau) = \frac{1}{N}\sum_{i=1}^{N} B_{\mathrm{loc},i}(t)B_{\mathrm{loc},i}(t+\tau) = \big\langle B_{\mathrm{loc}}(t)B_{\mathrm{loc}}(t+\tau)\big\rangle, \tag{15}$$

where i is a specific spin interacting with a certain local field, N is the total number of spins and it has been used the symbols $\langle\rangle$ to refer at the average of the product of the local fields. Even though the local field changes randomly over time as a result of the thermal motion, it does not depend from what point in time that local field is determined. Therefore the local fields fulfill the criteria for stationary random functions. [Keeler, 2011, p.253]

Even though the local fields do not depend from what point on time they have been determined, TCF depends on the time interval τ and therefore $G(t,\tau) = G(\tau)$. This means that if the time interval is zero, then $G(0) = \big\langle B_{\mathrm{loc}}(t)B_{\mathrm{loc}}(t)\big\rangle = \big\langle B_{\mathrm{loc}}^2\big\rangle$ is maximum. As the time interval increases, the local field changes randomly from its initial position and therefore its product with the local field in the beginning can be positive or negative which leads to a smaller $G(\tau)$ than $G(0)$. [Keeler, 2011, pp.254-255]

One of the simplest approximations to model Eq. 15 would be a single exponential as

$$G(\tau) = \big\langle B_{\mathrm{loc}}^2\big\rangle exp\left(\frac{-|\tau|}{\tau_c}\right), \tag{16}$$

where τ_{c} is the correlation time and the interval $|\tau|$ is in its absolute value to take into account any time interval, including a past time interval. It needs to be pointed out that the goal of doing MD simulations in this thesis, is to avoid such crude approximations, and thus, to get a more exact TCF with a molecular origin.

Returning to the previous simple approximation, Eq. 16, another way of defining the time correlation function is

$$G(\tau) = \big\langle B_{\mathrm{loc}}^2\big\rangle g(\tau), \tag{17}$$

where

$$g(\tau) = exp\left(\frac{-|\tau|}{\tau_{\mathrm{c}}}\right) \tag{18}$$

is the reduced correlation function and does not depend on the local fields. [Keeler, 2011, p.255]

3.5.1 Random motion and correlation time

The local field can be divided into the longitudinal component in the z direction and the transversal component in the plane xy. In order for the longitudinal relaxation to take place, the transversal component has to vibrate near the Larmor frequency around 10^9Hz. [Keeler, 2011, p.251]

A molecule can move in a couple different ways. In the first one, the molecule is vibrating and that means that the bond angles oscillate from their equilibrium position. This type of motion has an indirect influence on relaxation, but such influence is rather weak since its vibrational frequencies are about $10^{11} - 10^{13}$Hz which is much higher than the Larmor frequency. The other type of motion is rotation and for example, in a gas the molecules can rotate at frequencies of $10^8 - 10^9$Hz. For the liquids, even though there are many collisions, the movement of the molecules is quite restricted due to its high density and viscosity [Keeler, 2011, p.251]. The MD simulations time range are in orders of magnitude of nanoseconds, and thus, we are in the rotational frequencies of 10^9Hz and faster processes.

The rotational diffusion is the molecule's change of orientation from an initial z-axis due to constant collisions with other molecules. These collisions and consequently this type of motion are random and therefore the rotation is not steady and it can move back and forth. [Keeler, 2011, p.251]

The correlation time (τ_c) is the average time that a molecule needs to change its angle orientation 1 radian apart from its original location. Because the rotation has a certain range of frequencies, it is needed to quantify the amount of rotation that is exactly at the Larmor frequency. [Keeler, 2011, pp.252-253]

In this thesis molecular dynamic simulations have been done in order to determine the theoretical TCF for a monomer, dimer and trimer SDS molecules in water.

3.5.2 Spectral density and motional regimes

The spectral density, $J(\omega)$, is the Fourier transform of the TCF and it is used to quantify the amount of rotation that is actually at the Larmor frequency by placing $\omega = \omega_0$. In this thesis it is need to calculate the relaxation rates (Eq. 12 and 13). By taking the Fourier transform of the TCF, Eq. (16) gives:

$$G(\tau) = \left\langle B_{\text{loc}}^2 \right\rangle \exp\left(\frac{-|\tau|}{\tau_c}\right) \xrightarrow{\text{FT}} \left\langle B_{\text{loc}}^2 \right\rangle \frac{2\tau_c}{1+\omega^2\tau_c^2} = J(\omega) \tag{19}$$

The spectral density has a maximum at $\omega = 0$ and decreases as ω increases. On the other hand, the spectral density on the Larmor frequency, $J(\omega_0)$, for a dif-

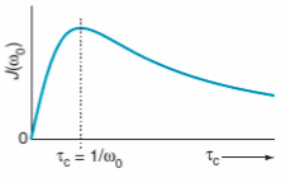

Figure 3: $J(\omega_0)$ vs τ_c. [Keeler, 2011, p.257]

ferent τ_c has a maximum when $\omega_0\tau_c = 1 \Rightarrow \tau_c = \frac{1}{\omega_0}$, as
it can be seen in Figure 3.

The fast motion regime is defined as $\omega_0\tau_c << 1$ and makes reference to the small molecules. For the reduced spectral density (without the amplitude), this implies the following approximation:

$$j(\omega_0) = \frac{2\tau_c}{1+\omega_0^2\tau_c^2} \approx 2\tau_c. \tag{20}$$

Therefore for the fast regime $j(\omega_0) = j(0)$. On the other hand, the slow motion regime is for bigger sized molecules such as large vesicles of the order of μm and $\omega_0^2\tau_c^2 >> 1$, which leads to

$$j(\omega_0) = \frac{2\tau_c}{1+\omega_0^2\tau_c^2} \approx \frac{2\tau_c}{\omega_0^2\tau_c^2} = \frac{2}{\omega_0^2\tau_c} = \frac{j(0)}{\omega_0^2\tau_c^2}. \tag{21}$$

[Keeler, 2011, pp.257-258]

3.6 Relaxation mechanisms

The relaxation mechanisms are sources of local magnetic fields due to different interactions between spins and the media and between spins themselves. There are many relaxation mechanisms but here we focus in the two most important ones concerning this study.

3.6.1 The dipolar mechanism

This is the mechanism that has already been discussed in which the local field comes from the magnetic moment from another spin. In this mechanism there are therefore two spins involved: the ones generating the field and the one interacting with it.

This local field has a $\frac{1}{r^6}$ dependency between the two spins and a dependence on natural constants as seen in Eq. 14. It is also important the angle between the two spin joining vector with the applied magnetic field, because it affects to the local field as well. [Keeler, 2011, p.249]

3.6.2 Chemical shift anisotropy

If the applied magnetic field is in the regime of a few tesla or more, the electrons in the molecule can produce a small induced field to the nucleus and therefore this last one experiences both, the applied and the induced field.

A chemical shift is anisotropic when the size of the induced field depends on the orientation of the molecule relative to the applied magnetic field. As a result of the chemical shift, the local field can be pointing in any direction, determined by the anisotropy of the electron distribution, and not just in the applied field's orientation. [Keeler, 2011, p.250]

4 Diffusion

In order to introduce the concept of *Diffusion*, first it is necessary to talk about the *Brownian motion*, which is the seemingly random movement of a particle in a solution caused by the collisions with the molecules from the media. Let's start with the average unidimensional kinetic energy of a particle along the x-axis as being

$$\langle E \rangle = \left\langle \frac{mv_x^2}{2} \right\rangle = \frac{kT}{2}, \tag{22}$$

from where it can be obtained that $\langle v_x^2 \rangle = \frac{kT}{m}$. In a random walk three criteria are fulfilled. Firstly the distance travelled at each step is $\delta = \pm v_x \cdot \tau$, where $\pm v_x$ is the velocity of the particle and τ is the time step. Secondly it has to be taken into account that the probability of the particle going to either direction is $\frac{1}{2}$ and each step does not depend of the previous one. Lastly each particle in the solution moves independently of all the other particles. [Berg, 1993, pp.5-7]

In a random walk, the average particle position is zero. Let's consider N particles and let the position of the particle i at the step n be $x_i(n) = x_i(n-1) \pm \delta$. The mean displacement of the particles after the nth step goes according

$$\langle x(n) \rangle = \frac{1}{N} \sum_{i=1}^{N} x_i(n) = \frac{1}{N} \sum_{i=1}^{N} (x_i(n-1) \pm \delta) = \frac{1}{N} \sum_{i=1}^{N} x_i(n-1) = \langle x(n-1) \rangle, \tag{23}$$

where the mean of $\pm\delta$ vanishes because about half of the particles have the positive sign and the other half negative. This implies that the mean position of the particles do not change with the steps and that the particles spread symmetrically from that mean position which can very well be considered the origin. [Berg, 1993, pp.7-8]

The spreading of the particles can be measured with the root-mean-square displacement as follows:

$$\begin{aligned} & x_i^2(n) = (x_i(n-1) \pm \delta)^2 = x_i^2(n-1) \pm 2\delta x_i(n-1) + \delta^2, \\ & \langle x^2(n) \rangle = \frac{1}{N} \sum_{i=1}^{N} x_i^2(n) = \frac{1}{N} \sum_{i=1}^{N} [x_i^2(n-1) \pm 2\delta x_i(n-1) + \delta^2] = \\ & \langle x^2(n-1) \rangle + \delta^2, \end{aligned} \tag{24}$$

and again the middle term averages to zero. If it is considered the origin where the mean position of the particles is located, then at $n = 0$, $x_i(0) = 0$ for all particles i

and thus $\langle x^2(0)\rangle = 0$. Therefore

$$\begin{cases} \langle x^2(1)\rangle = \langle x^2(1-1)\rangle + \delta^2 = \delta^2, \\ \langle x^2(2)\rangle = \langle x^2(1)\rangle + \delta^2 = 2\delta^2, \\ . \\ . \\ . \\ \langle x^2(n)\rangle = n\delta^2. \end{cases} \tag{25}$$

Since for each step it takes τ seconds, it will take $t = n\tau$ seconds to move n steps and the mean-squared displacement can be written as

$$\langle x^2(t)\rangle = \left(\frac{t}{\tau}\right)\delta^2 = \left(\frac{\delta^2}{\tau}\right)t, \tag{26}$$

where it can be written $x(t)$ instead of $x(n)$ because x is a time function variable. Hence

$$\langle x^2(t)\rangle = \left(\frac{\delta^2}{\tau}\right)t = 2\cdot\frac{1}{2}\cdot\left(\frac{\delta^2}{\tau}\right)t = 2Dt, \tag{27}$$

where $D = \frac{1}{2}\cdot\left(\frac{\delta^2}{\tau}\right)$ is the diffusion coefficient. Similarly, for more dimensions it is equally valid that $\langle y^2\rangle = 2Dt$ and $\langle z^2\rangle = 2Dt$ and therefore in three dimensions $\langle r^2\rangle = \langle x^2\rangle + \langle y^2\rangle + \langle z^2\rangle = 6Dt$. [Berg, 1993, pp.9-11]

The diffusion is therefore the movement of particles driven by the Brownian motion through a media. In a short time scale there are many interactions between the molecules due to thermal motion which affect the random walk and therefore the diffusion coefficient as it has been presented in Eq. (27). For this reason the diffusion coefficient is useful for the long time limit according to

$$D = \lim_{t\to\infty}\frac{\langle \Delta r^2(t)\rangle}{6t}, \tag{28}$$

where it is written Δr instead of just r in a more general form, where it is considered any origin.

4.1 Stokes-Einstein equation and hydrodynamic radius

Another way to approach the diffusion coefficient is through the Stokes-Einstein equation. This equation was derived by Einstein from Fick's laws considering the Brownian movement of the particles in a dilute liquid phase giving a diffusion coefficient of $D^0 = \frac{kT}{f}$, where f is the frictional coefficient of the particle. Stokes showed then that, for a spherical particle of radius r moving with a velocity v, the frictional coefficient

is $f_0 = 6\pi\eta r$, where η is the fluid viscosity. Therefore for the special case of spherical molecules

$$D^0 = \frac{kT}{6\pi\eta r}, \tag{29}$$

known as Stokes-Einstein (SE) equation [Edward, 1970, p.261]. In this thesis, the diffusion coefficient obtained with this approximation is compared with the one obtained through the MSD with the MD simulations. In other words, here it is explored the validity of Eq. 29 with a more exact diffusion coefficient by using computational tools.

This equation has several limitations starting with that most of the molecules are not spherical. Another problem is that the SE equation assumes that the fluid is continuous and is always in contact with the solute molecules or particles. This is true as an approximation for large molecules or aggregations, but for small molecules the liquid cannot be considered any more continuous and the SE equations need empirical correction factors for very small molecules. In the particular case of this thesis, the molecule studied can be considered large enough to assume a continuous contact with the solvent molecules.[Edward, 1970, pp.261-262]

To deal with the non-sphericity of most molecules, it has been widely discussed in the literature different approaches to use the SE equation, by changing the definition of the molecule radius. The first one is the van der Waals radius r_ω, which pictures the molecule enclosed by a van der Waals surface, limiting how close can a molecule be from another one. Another way to obtain the radius is from molecular drawings r_{mod}, and it turns out to be a bit larger than r_ω but it is harder to calculate, since all the axes and angles have to be taken into consideration. Since the r_ω takes into consideration the sum of all the individual spheres enclosing each atom of the molecule, in between each enclosed atom can be some free space. If this space is taken into account, it can be calculated the molecular volume by dividing the molar volume with the Avogadro's number, $v_M = \frac{V_M}{N}$. With the molecular volume it can be easily obtained the molecular radius which is even bigger than r_{mod}. [Edward, 1970, pp.262-264]

The general term for these kind of radius which treat the molecules as if they were perfect spheres is hydrodynamic radius, and in this particular thesis it has been calculated by taking the ensemble average over all the atoms of the polymer chain using the following equation:

$$\frac{1}{R_{\mathrm{H}}} = \left\langle \frac{1}{|\mathbf{r}_m - \mathbf{r}_n|} \right\rangle, \tag{30}$$

where $|\mathbf{r}_m - \mathbf{r}_n|$ is the vectorial distance between the atoms m and n. The symbols $\langle\rangle$ are used once again to denote that the ensemble average or just average is taken. This gives a R_H a bit smaller than the r_ω calculated according the literature.[Teraoka, 2002, p.186]

The hydrodynamic radius is also useful to calculate the *rotational correlation time*

as

$$\tau_r = \frac{4\pi\eta R_H^3}{3k_B T}, \tag{31}$$

where k_B is the Boltzmann constant. [arne.b, 2016][Braslavsky et al., 2007, p.416]

4.2 Error for the mean square displacement

From simulations, in order to determine the diffusion coefficient (Eq. 28) as well as to get the relaxation rates, it is needed a considerable amount of statistical data for the successful representation of the mean square displacement versus time. It is therefore necessary to display the results with certain uncertainty or associated error, to be able to compare it with the theoretical model. When the intention is to compare the experimental or simulated mean square displacement with the model graphically, the error bars are commonly used.

The error bars represent the error of the mean square displacement with one standard error from above and below giving about 68% of confidence. The error has been calculated by using the standard deviation according to

$$\epsilon = \frac{\sigma}{\sqrt{N}}, \tag{32}$$

where σ is the standard deviation and N is the population or the number of data sets.[Sylvia Wassertheil-Smoller, 1995, pp.40-41] [E.Kloeden and Platen, 1999, p.46]

The goal for the standard error is to become smaller as the sample amount increases according to Eq. (32). The reason for using the standard deviation is to estimate how far the sample mean is from the whole population mean. The sample mean refers to the mean square displacement of each data set and the population mean to the mean of the samples.

5 Simulation modelling

Figure 4: Flow chart for an SDS simulation

In this chapter, it is explained in a broad manner the steps and considerations followed to carry out a SDS simulation with the help of a flow chart (Figure 4). The goal of these simulations is to end up with enough statistical data to succesfully extract a mean square displacement and a TCF.

In the step 1 (Figure 4) of a SDS simulation, it was needed to draw the molecule. After that, in step 2 it was calculated the atomic charges, molecular topology and the potential energy from the system of atoms conforming the molecule. In step 3 it was added the solvent in order to study the interactions of the SDS molecule within it. In this same step it was stripped a sodium atom, because the molecule is in its ion form in a water solution.

After adding the solvent, an energy minimization on the system took place in the step 4 of the chart. This step was carried out until the system's energy reached its minimum and did not change. This step can take some minutes to simulate.

Next starts the heating in step 5, where the system's temperature was slowly increased from 0 K to 288 K. In this step it was simulated the system for 30 picoseconds. This step might take roughly half an hour to complete.

The pressure step is the step 6 from the chart (Figure 4), where it was assumed that the system was in a thermal bath set at 293 K and after that the temperature remained constant. The goal here was to simulate the system at a constant pressure of 1 bar. The whole system was allowed to evolve with this conditions for about 300 picoseconds, which took about 5 h of simulation.

The step 7 in the flow chart (Figure 4) is the final step of the simulation. Here the pressure and temperature were kept constant as well as the system's volume. In order for the whole system to stabilize it

was necessary to simulate about 2000 picoseconds, which took a couple of simulation days.

Once the volume phase (step 7) was finished, it was extracted the molecule's mean square displacement throughout the 2 nanoseconds of simulation, and plotted it according with Eq. (28) to obtain the diffusion coefficient. The problem comes when the statistical error is too high to be able to extract any meaningful information from the mean square displacement. In this case, step 7 needs to be repeated several times to reduce the error according to Eq. (32), and thus succeeding to get a trend for the diffusion.

In order to carry out the SDS modelling, the Amber molecular dynamics package simulator [Case et al., 2016] was used.

In order to calculate the mean square displacement for the monomer, dimer and trimer, it has been needed to take first the $\langle \Delta r^2 \rangle$ from 8 data sets (4 simulations with 2 nanosecond length each) for the monomer and trimer, each of which representing a 1 nanosecond simulation, and 3 data sets for the dimer with the same time length. After that it has been taken the mean of all data sets for each case obtaining the mean of the mean square displacement. The reason for which the dimer contains less amount of data, is that during the simulation it was found that the two lipids did no stick together for certain intervals, and in order to have reliable data it was necessary to remove such periods of time.

For the case of the TCF, the rotational correlation time or τ_r can be calculated by fitting an exponential curve with the parameters adjusted using the SE equation for the rotational diffusion, as in Eq. (31).

6 Results and discussion

In this chapter, it is compared a model with parametrized R_H from Eq. (29) and Eq. (31) versus a complete simulated results of the mean square displacement and TCF.

6.1 Model vs simulation

The model mean square displacement is calculated using the Stokes-Einstein's equation (29) by taking advantage of the hydrodynamic radii, Eq. (30), which are listed in the Table (1):

Table 1: Hydrodynamic radius for the monomer, dimer and trimer

	R_H (Å)	$\epsilon(R_H)$(Å)
1 SDS	3.702	0.004
2 SDS	5.077	0.081
3 SDS	5.633	0.026

As it is expected, the hydrodynamic radius increases as more molecules combine together forming bigger aggregates. Nevertheless, it has to be pointed out that there is not such a big difference from the dimer's to the trimer's R_H. It's plausible to think that this is because the SDS molecule is really flexible and it tends to form packed aggregates.

The slope from the model is calculated according to the mean square displacement $\langle \Delta r^2 \rangle$ (Eq. 28), where the diffusion coefficient D is the one calculated by using the SE equation (29) with the R_H from the Table (1). In Figure 5, it is represented the simulated and modelled mean square displacement for the three cases with the error bars.

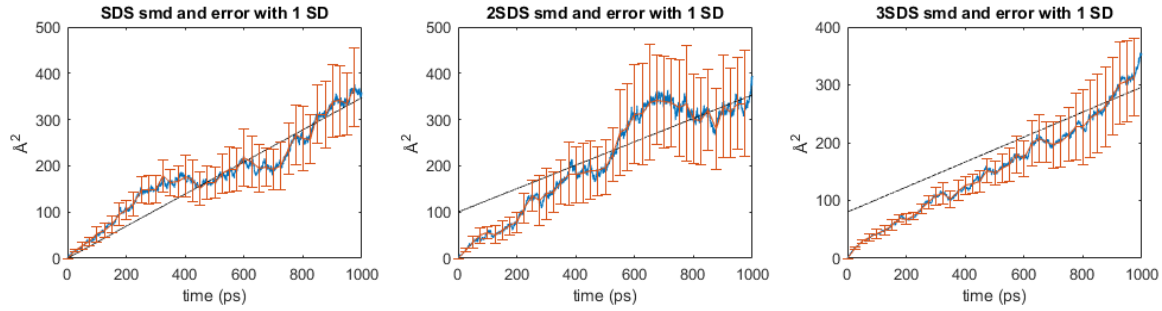

Figure 5: Experimental and theoretical MSD (smd) for the three cases with one standard deviation (1 SD) error

The limit in Eq. (28) is approximated with the tail of the simulated $\langle \Delta r^2 \rangle$. As it can be observed in Figure 5, the theoretical mean square displacement does not intersect the origin. This is because it has been manually adjusted in order to match the long time tail of the simulated MSD according to the SE equation (Eq. 29). It is thus observed that the theoretical mean square displacement has the same trend as the tail of the simulated one within the error bars. This fact suggests that the simulation do not disagree with the theory and it is therefore plausible to consider the hydrodynamic radius to calculate the lipid's diffusion in water, at least up to a trend in aggregate size versus diffusion.

As it has been commented in the simulation modelling section, the dimer contains less amount of statistical data and this is reflected in the error bars of Figure 5. It can be observed that the error for the dimer is much higher than in the other two cases.

Up until now it has been discussed how the simulated mean square displacement behaves and the fact that it is in agreement with the theoretical mean square displacement using the hydrodynamic radius. Another way to test the usefulness of the hydrodynamic radius is through the rotational time correlation function (TCF).

The next picture (Figure 6) shows the simulated TCF for the monomer (left) and for the dimer and trimer (right) with their respective adjusted exponential.

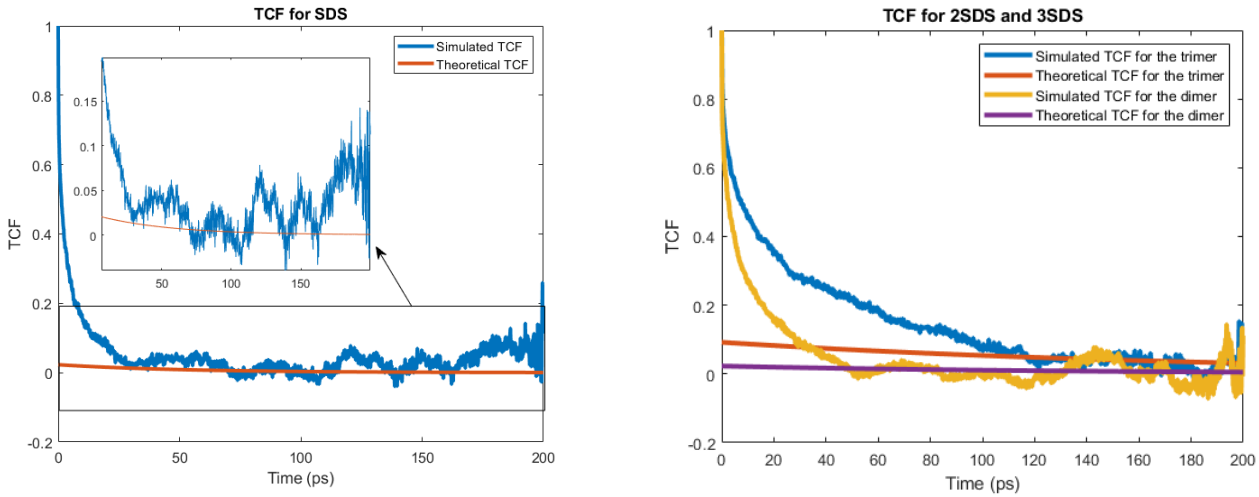

Figure 6: Left: TCF for the monomer. Right: TCF for the dimer and trimer

In order to calculate the τ_c, the TCF is adjusted by using three exponentials with the form $a_i e^{\left(-\frac{t}{\tau_i}\right)}$. After applying the FT and since this molecule is in the fast regime, the fitted correlation time can be calculated by using $\tau_c = a_1\tau_1 + a_2\tau_2 + a_3\tau_r$, where a_1, a_2, τ_1 and τ_2 were obtained with a fit and τ_r is the rotational correlation time for each case. Also a_3 has been adjusted to fit the long tail limit in (Figure 6).
The simulated TCF (Figure 6) has been normalized to start at 1 and the theoretical curve has been adjusted accordingly by using Eq. (16). The normalization is done in

order to be able to compare the three cases. For the previous figure the τ_r used for the theoretical curve is $\tau_r^{(1)} = 52.6$ ps, $\tau_r^{(2)} = 135.7$ ps and $\tau_r^{(3)} = 218.1$ ps for each case respectively, which has been calculated by using the R_H according to the Table (1). The adjusted rotational TCF amplitude for the monomer and the dimer is $a_3 = 0.023$ and for the trimer is five times larger. In the zoomed version of the figure 6 (left), can be observed that the decaying time of the monomer is $\tau_r^{(1)}$.

The rotational theoretical TCF for the three cases in the previous figure (Figure 6) has been adjusted for the tail of the simulated TCF respectively. It can be therefore observed that in all the cases the simulated results agree with the theoretical ones using the hydrodynamic radius. Hence the usefulness of the R_H is backed up by using two different approaches, the mean square displacement and the TCF.

From the right case of the picture above (Figure 6), it can be observed that the dimer's TCF decays faster than the trimer's case, and that is because the trimer is a bigger aggregate than the dimer and therefore it takes more time for the trimer to rotate through the media.

6.2 Relaxation times

In order to show that the SDS molecule is in the fast motion regime, it is necessary to check that $\omega_0\tau_c << 1$ as stated previously in Section 3.5.2. This is quite simple to check, since the correlation time is in the order of magnitude of picoseconds $\approx (10^{-12}\text{s})$, and for the Larmor frequency it is used $\omega_0 = -\gamma B_0$ [Keeler, 2011, p.32], where $B_0 = 11.09$ T is the usual applied magnetic field and $\gamma_H = 267.52 \cdot 10^6 \frac{\text{rad}}{\text{sT}}$ is well known for the proton. This gives a value for ω_0 in the order of $\approx 10^9$, which implies that indeed is the case $\omega_0\tau_c << 1$.

For the calculation of T_1 has been used the Eq. (12), where r_{eff} is explicitly obtained by MD by looking at the amplitude of the time correlation function $\langle B_{\text{loc}}^2 \rangle$. For the calculation of T_2 is used Eq. (13).

The simulated relaxation times for the monomer, dimer and trimer are displayed in the Table 2.

Table 2: Model relaxation times for each case

	T_1 (s)	$\epsilon(T_1)$(s)	T_2 (s)	$\epsilon(T_2)$(s)
1 SDS	4.607	0.255	4.525	0.250
2 SDS	1.531	0.153	1.442	0.170
3 SDS	0.956	0.012	0.588	0.008

As it can be seen in the Table 2, T_1 and T_2 relaxation times are really similar for each case, which backs up the fact that the molecule is in the fast motion regime,

because in the extreme narrowing limit the two decay times are the same. For the trimer, the relaxation times (T_1 and T_2) differ considerably compared with the other two cases, which means that the molecule is much bigger.

6.3 Comparison with experiments

While discussing the simulated mean square displacement (Figure 5), it was mentioned that it has the same trend than the theoretical one. That fact suggests that the simulated results agrees with the theory and therefore, it is reasonable to use the theoretical model to get some specific value for the diffusion coefficient. In this case it can be used the already obtained hydrodynamic radius with the SE equation (29) to calculate the diffusion coefficient for each case as shown in Table 3.

Table 3: Model diffusion coefficients for each case with the associated error

	$D \cdot 10^{10}(\mathrm{m}^2/\mathrm{s})$	$\epsilon(D) \cdot 10^{10}(\mathrm{m}^2/\mathrm{s})$
1 SDS	4.6	0.01
2 SDS	3.4	0.1
3 SDS	2.9	0.2

The tabulated values are quite reasonable for a really low SDS concentration in water, since it agrees with certain literature such as $D_{\mathrm{bib}}^{(1)} = 6.9{\cdot}10^{-10}\ \frac{\mathrm{m}^2}{\mathrm{s}}$ [Yuan et al., 2001] and $D_{\mathrm{bib}}^{(2)} = 4.3 \cdot 10^{-10}\ \frac{\mathrm{m}^2}{\mathrm{s}}$ [Olle Söderman, 2004].

The bibliographical value for the transverse relaxation time is $T_2 = 1.248\,\mathrm{s}$ [Yuan et al., 2001] which is quite similar with the dimer's simulated value of $T_2^{\mathrm{dimer}} = 1.442\,\mathrm{s}$, but it differs considerably from the other two cases. A possible reason for such a difference is that here it has been studied the cases of the monomer, dimer and trimer, but in an actual laboratory experiment the sample contains a mixed amount of aggregations. Despite the discrepancy with the literature, the diffusion coefficients and relaxation constants obtained in this thesis are quite plausible, since they are not off by any order of magnitude compared with the bibliography.

7 Conclusions

Initially it was proposed the possibility of using the molecule's hydrodynamic radius in the Stokes-Einstein equation in order to obtain a modelled mean square displacement and if it would agree with the one obtained by the MD simulations, which do not depend on the SE equation. After comparing the results in Figure 5, it is plausible to say that the trend of the simulated mean square displacement do not disagree with the one obtained from the hydrodynamic radius within certain error. Therefore it would be possible to extract the SDS molecule's diffusion coefficient by just using the Stokes-Einstein model and computed R_H instead of having to go through all the simulations.

To back up the results discussed in the previous paragraph, the dipole-dipole time correlation function has been simulated for the monomer, dimer and trimer and compared with the model by using again the hydrodynamic radius. The correspondent graphic is found in Figure 6 and again, as it is observed in the long trajectory, both experimental and theoretical results agree. This fact provides further evidence of the usefulness of using the molecule's hydrodynamic radius to calculate the molecule's rotational diffusion coefficient in water.

The simulated SDS diffusion coefficient, of a low concentration surfactant in a water solution, obtained in this work is of $D = 4.6 \cdot 10^{-10} \frac{\mathrm{m}^2}{\mathrm{s}}$ in the monomer case. Compared to the bibliographical values of $D_{\mathrm{bib}}^{(1)} = 6.9 \cdot 10^{-10} \frac{\mathrm{m}^2}{\mathrm{s}}$ [Yuan et al., 2001] and $D_{\mathrm{bib}}^{(2)} = 4.3 \cdot 10^{-10} \frac{\mathrm{m}^2}{\mathrm{s}}$ [Olle Söderman, 2004], we can conclude that they are within the same order of magnitude and thus, not in disagreement. Similarly, the transversal relaxation time simulated for the dimer is $T_2^{\mathrm{dimer}} = 1.442\,\mathrm{s}$, which compared with the literature, $T_2 = 1.248\,\mathrm{s}$ [Yuan et al., 2001], it is also within the same order of magnitude.

In conclusion, the use of the R_H and the Stokes-Einstein equation is not just limited to get the molecule's diffusion coefficient, but is also useful to easily obtain the dipole-dipole relaxation rates. This would therefore be of great help, since it would considerably reduce the simulation time and resources.

References

[arne.b, 2016] arne.b (2016). Relation of translational and rotational diffusion of a spherical particle. `https://physics.stackexchange.com/q/277481`. [Online; accessed 24-August-2019].

[Berg, 1993] Berg, H. C. (1993). *Random walks in biology*. Princeton University Press.

[Braslavsky et al., 2007] Braslavsky, S., Acuña, A., Adam, W., Amat, F., Armesto, D., Atvars, T., Bard, A., Bill, E., Björn, L., Bohne, C., Bolton, J., Bonneau, R., Bouas-Laurent, H., Braun, A., Dale, R., Dill, K., Döpp, D., Dürr, H., Chanon, M., and Zachariasse, K. (2007). Glossary of Terms Used in Photochemistry, 3rd edition (IUPAC Recommendations 2006). *Pure and Applied Chemistry*, 79:293–465.

[Case et al., 2016] Case, D., R.M. Betz, D. C., T.E. Cheatham, I., T.A. Darden, R. D., T.J. Giese, H. G., A.W. Goetz, N. H., S. Izadi, P. J., J. Kaus, A. K., T.S. Lee, S. L., P. Li, C. L., T. Luchko, R. L., B. Madej, D. M., K.M. Merz, G. M., H. Nguyen, H. N., I. Omelyan, A. O., D.R. Roe, A. R., C. Sagui, C. S., W.M. Botello-Smith, J. S., R.C. Walker, J. W., R.M. Wolf, X. W., Xiao, L., and (2016), P. K. (2016). AMBER 2016, University of California, San Francisco. `http://ambermd.org/index.php`. [Online; accessed 4-September-2019].

[Edward, 1970] Edward, J. T. (1970). Molecular volumes and the Stokes-Einstein equation. *Journal of Chemical Education*, 47(4):261.

[E.Kloeden and Platen, 1999] E.Kloeden, P. and Platen, E. (1999). *Numerical Solution of Stochastic Differential Equations*. Springer.

[Joseph P. Hornak, 1997] Joseph P. Hornak (1997). The basics of NMR. `https://www.cis.rit.edu/htbooks/nmr/inside.htm`. [Online; accessed 9-August-2019].

[Jozef Kowalewski, 2006] Jozef Kowalewski, L. M. (2006). *Nuclear spin relaxation in liquids: Theory, experiments, and applications*. Taulor & Francis.

[Keeler, 2011] Keeler, J. (2011). *Understanding NMR spectroscopy*. John Wiley & Sons.

[NASA earth observatory, 2010] NASA earth observatory (2010). Aerosols and Incoming Sunlight (Direct Effects). `https://earthobservatory.nasa.gov/features/Aerosols/page3.php`. [Online; accessed 22-May-2020].

[Olle Söderman, 2004] Olle Söderman, Peter Stilbs, W. S. P. (2004). NMR studies of surfactants. *Concepts in Magnetic Resonance*, 23A(2):121–135.

[Sylvia Wassertheil-Smoller, 1995] Sylvia Wassertheil-Smoller (1995). Biostatistics and Epidemiology. `https://books.google.fi/books?id=-PHiBwAAQBAJ&pg=PA40&redir_esc=y#v=onepage&q&f=false`. [Online; accessed 22-August-2019].

[Teraoka, 2002] Teraoka, I. (2002). *Polymer solutions: an introduction to physical properties*. John Wiley & Sons.

[Wennerström, 1999] Wennerström, H. (1999). *The colloidal domain: where physics, chemistry, biology, and technology meet*. Wiley-VCH.

[Yuan et al., 2001] Yuan, H., L. Luo, L. Z., S. Zhao, S. M., J.Y. Yu, L. S., and Du, Y. (2001). Aggregation of sodium dodecyl sulfate in poly(ethylene glycol) aqueous solution studied by ^1H NMR spectroscopy. *Colloid Polym Sci*, 280:479–484.

[Zhao and Fung, 1993] Zhao, J. and Fung, B. M. (1993). NMR study of the transformation of sodium dodecyl sulfate micelles. *Langmuir*, 9(5):1228–1231.